

Effects of High Water-Vapor Pressure on Oxidation of Silicon Carbide at 1200°C

Peter F. Tortorelli* and Karren L. More*

Metals and Ceramics Division, Oak Ridge National Laboratory, Oak Ridge, Tennessee 37831

The oxidation of SiC at 1200°C in a slowly flowing gas mixture of either air or air + 15 vol% H₂O at 10 atm (1 MPa) was studied for extended times to examine the effects of elevated water-vapor pressure on oxidation rates and microstructural development. At a water-vapor pressure of 1.5 atm (150 kPa), distinct SiO₂ scale structures were observed on the SiC; thick, porous, nonprotective cristobalite scales formed above a thin, nearly dense vitreous SiO₂ layer, which remained constant in thickness with time as the crystalline SiO₂ continued to grow. The pore morphology of the cristobalite layer differed depending on the type of SiC on which it was grown. The crystallization and growth rates of the cristobalite layer were significantly accelerated in the presence of the high water-vapor pressure and resulted in rapid rates of SiC surface recession that were on the order of what is observed when SiO₂ volatility is rate controlling at high gas-flow velocities (30 m/s). The recession process can be described by a parabolic kinetic model controlled by the conversion of dense vitreous SiO₂ to porous, nonprotective SiO₂.

I. Introduction

THE effects of water vapor on the high-temperature oxidation of silicon-based ceramics in high-temperature air or oxygen have been investigated for many years (see, for example, Refs. 1–12). A principal effect is the influence of water vapor on the parabolic rate constant (k_p) that often governs the growth of SiO₂ on SiC:

$$x^2 = k_p t \quad (1)$$

where x is the thickness of the oxide product and t the oxidation time. As shown by Deal and Grove for silicon¹ and as extensively characterized by Opila⁸ for SiC, water vapor significantly increases k_p , even at relatively low concentrations in the environment, through its direct influence as an oxidant. Fundamentally, this is because k_p is dependent on the product of oxidant diffusivity (D) and solubility (C) in the growing oxide and, while D for H₂O in SiO₂ is somewhat less than that of oxygen, C is substantially higher, such that⁵

$$\frac{k_p(\text{H}_2\text{O}, \text{SiO}_2)}{k_p(\text{O}_2, \text{SiO}_2)} = \sim 50 \quad (2)$$

Another effect of water vapor relates to the formation of volatile products, such as Si(OH)₄, by its direct reaction with SiO₂.^{7,10} Under conditions where significant volatility of the SiO₂ can occur, the SiO₂ can grow by the solid-state oxidation process

governed by k_p , but, after a certain time, its thickness is limited by the simultaneous loss of SiO₂ by formation of gaseous products. These coupled reactions can be described by parabolic oxidation kinetics in terms of k_p and a linear rate constant (k_l) related to the volatilization rate of the SiO₂.⁵ The equilibrium SiO₂ layer is created at the same rate it is removed by formation of the volatile products, and the underlying ceramic is consumed at a linear (recession) rate set by k_l . Because k_l is related to the volatilization rate, it should be dependent on the velocity and pressure of the oxidizing gas in well-prescribed ways. This relationship has been recently rigorously demonstrated experimentally for SiC.⁹

From a practical viewpoint, the effects of water vapor on high-temperature oxidation form an important area of study for combustion applications where water-vapor partial pressures ($p_{\text{H}_2\text{O}}$) can be quite significant. For gas turbines with high pressure ratios, values of $p_{\text{H}_2\text{O}}$ are higher than those encountered in most oxidation experiments; relatively few laboratory studies have been conducted at water-vapor pressures > 1 atm. Furthermore, most exposures at high water-vapor pressures have been for short times (≤ 100 h). Consequently, as part of an effort to characterize and understand environmental effects on SiC-based composites at the higher system pressures and longer operating times typical of combustion conditions in land-based gas turbines, the oxidation of various silicon carbides and silicon in air + 15 vol% H₂O at 10 atm (1 MPa) has been studied for exposures up to 4000 h. The present work is for the case where the water-vapor pressure is high and the gas velocity is low.^{11,12} This paper addresses the effect of water vapor on the oxidation of SiC (and material recession based on such) in the absence of significant loss of SiO₂ by volatilization, which, as described above, is the dominant controlling recession mechanism at high gas velocities.^{9,10}

II. Experimental Procedures

Bars (~50 mm × 4 mm × 3 mm) or thin plates (~40 mm × 10 mm × 3 mm) of SiC and silicon were exposed at 1200°C to slowly flowing (typically, ~3 cm/min, but, in one case, 18 cm/min) air or air + 15% H₂O at a total pressure of 10 atm, typically in 500 h increments. Multiple specimens were hung vertically from a slotted pure Al₂O₃ holder (Cortek, Inc., Golden, CO) inside an 8 cm ID sintered α-SiC (Hexoloy™ SA, The Carborundum Co., Niagara Falls, NY) closed-end tube (~1 m long) that served as the pressure vessel. The α-SiC tubes were externally heated by SiC heating elements encased in a large refractory-lined box. The oxidizing gas was delivered to the bottom of the SiC tube through a preoxidized 0.5 cm OD tube fabricated from an Al₂O₃-forming alloy and flowed upward past the specimens.

To study the effects of water vapor on high-temperature oxidation, pure water was injected into the high-purity compressed-air stream and flashed to vapor. Water injection was by means of a calibrated-volume mechanical pump. The water was condensed from the gas after it exited the reaction zone; its volume was measured (usually every 24 h) and, combined with flow velocity determination, used to monitor and control the water-vapor concentration. The water-vapor concentration was controlled by changing the injection volume and/or frequency of the

E. J. Opila—contributing editor

Manuscript No. 186661. Received October 30, 2002; approved April 4, 2003. Presented at the Symposium on Water Vapor Effects on Oxidation of High-Temperature Materials at the 131st Annual Meeting of the Minerals, Metals, and Materials Society (TMS), Seattle, WA, February 18–20, 2002.

*Member, American Ceramic Society.

pump as appropriate or by adjusting the carrier-gas velocity. Sufficient gas volume was used so that little change (less than ~1%) in the water-vapor concentration occurred because of reaction with the specimens and SiC tube. Additional details regarding the high-temperature, high-pressure experimental facility can be found elsewhere.^{6,11}

The SiC materials used in this study were sintered α -SiC (Hexoloy SA) and high-purity β -SiC produced by chemical vapor deposition (CVD). The CVD-SiC was exposed in bulk form (Morton International Advanced Materials, Woburn, MA) or as a thick (>200 μm) seal coat on SiC-fiber-reinforced SiC composites (General Electric Power Systems Composites, LLC, Newark, DE). Specimens of pure semiconductor-quality silicon (obtained from H. Wang of General Electric Power Systems) were simultaneously oxidized in some experiments.

X-ray diffractometry (XRD; Model Scintag Pad V, Thermo ARL, Dearborn, MI) was used to determine the phase and extent of crystallinity of reaction products on the surfaces of exposed specimens. Polished cross-section specimens were characterized using backscattered electron (BSE) imaging and associated microchemical analysis using electron probe microanalysis (Model 733, JEOL USA, Inc., Peabody, MA). Specimens for analysis by transmission electron microscopy (TEM) were prepared using the focused-ion-beam (FIB) technique (Model FB-2000A, Hitachi Scientific Instruments, Tokyo, Japan) and subsequently examined using field-emission-gun TEM (Model HF-2000, Hitachi Scientific Instruments). Mass change and oxide thickness were found to not accurately reflect the extent of oxidation reaction because of irregular loss of friable or loosely adherent reaction products during specimen handling. Consequently, the degree of degradation by oxidation was determined from posttest microstructural analysis and measurement of the SiC recession directly from the polished cross sections.

III. Results

Exposure of SiC to air + 15% H_2O at 1200°C and 10 atm always resulted in the formation of a thick, porous SiO_2 scale on the specimen surfaces. An example of such for α -SiC is shown in Fig. 1(a). In contrast, if the same SiC was exposed to only air at 1200°C and 10 atm, the extent of oxidation was much less (Fig. 1(b)). Similarly, CVD-SiC showed extensive SiO_2 formation when water vapor was present in the environment. As shown in Fig. 2(a), CVD-SiC oxidized in air + 1.5 atm (150 kPa) H_2O at 1200°C for 500 h also exhibited a thick porous SiO_2 product, but this layer was morphologically different from that formed on the identically exposed α -SiC (Fig. 2(b)). XRD of numerous specimen surfaces of CVD-SiC and α -SiC after exposures to the air + 1.5 atm H_2O environment for ≥ 100 h consistently identified the thick, porous surface SiO_2 layer as cristobalite. The porous cristobalite scales

that formed on the silicon carbides exposed to air + 1.5 atm H_2O environment continually thickened with exposure time (Fig. 3).

A thin, denser SiO_2 layer adjacent to the SiC was typically observed under the much thicker, porous SiO_2 scales. The arrows in Figs. 1(a) and 2 indicate this layer, which was always distinct on oxidized CVD-SiC specimens, but was more difficult to clearly observe on the α -SiC because of the typical roughness of the interfaces between the outer and inner products and between the oxide and the carbide. Pores apparently were sometimes observed in this underlying layer on the α -SiC, but their precise location was difficult to determine because of the irregular interfaces in this system. Two-layer scale morphologies have been reported previously¹² and have been observed under similar exposure conditions for CVD-SiC seal coats used to protect SiC-based, fiber-reinforced composites.¹¹

Cross-section TEM of FIB-prepared CVD-SiC exposed for 500 h revealed that the thin underlying layer was fully dense vitreous SiO_2 , as shown in Fig. 4. This layer was typically 4–6 μm thick. Precise thickness determinations were limited by interfacial roughness and microstructural differences among the various forms of SiC. However, in contrast to the outer product, which thickened with exposure time, no significant change in the thickness of this vitreous SiO_2 layer on any of the CVD-SiC or α -SiC specimens over 100–4000 h of exposure time was observed. This is shown in Fig. 3, where a structurally distinct underlying microlayer has a similar thickness at 100 and 3500 h of exposure. A clearer example of the constancy of the thickness of the vitreous layer is shown in Fig. 5, which compares cross-sectional images of a CVD-SiC seal coat on a SiC/SiC composite after 500 and 3500 h of exposure at 1200°C in air + 1.5 atm H_2O . Substantial recession of the SiC has occurred between 500 and 3500 h; however, the vitreous SiO_2 layer has not thickened.

Pure silicon was also exposed to air + 1.5 atm H_2O at 1200°C and exhibited a similar two-layer oxide structure consisting of cristobalite overlying a thinner vitreous SiO_2 , as shown by the BSE and TEM images in Figs. 6 and 7, respectively. However, unlike the reaction products observed on the different silicon carbides, the cristobalite that formed on pure silicon during exposure to a high $p_{\text{H}_2\text{O}}$ was dense. Only a few isolated large pores were observed in the cristobalite that formed on the silicon, and they were microstructurally distinct from those in the crystalline SiO_2 on the silicon carbides (Figs. 1 and 2).

Continual exposure in the air + 1.5 atm H_2O environment resulted in relatively rapid recession (loss) of SiC by oxidation, as clearly shown in Fig. 5. Because reliable measurements of cristobalite thickness were not always possible because of oxide spallation during either cooling or handling, direct measurement of SiC recession was used to experimentally determine oxidation rates. This was done by careful determination of the thickness of the remaining unreacted SiC (x) from imaging of polished cross

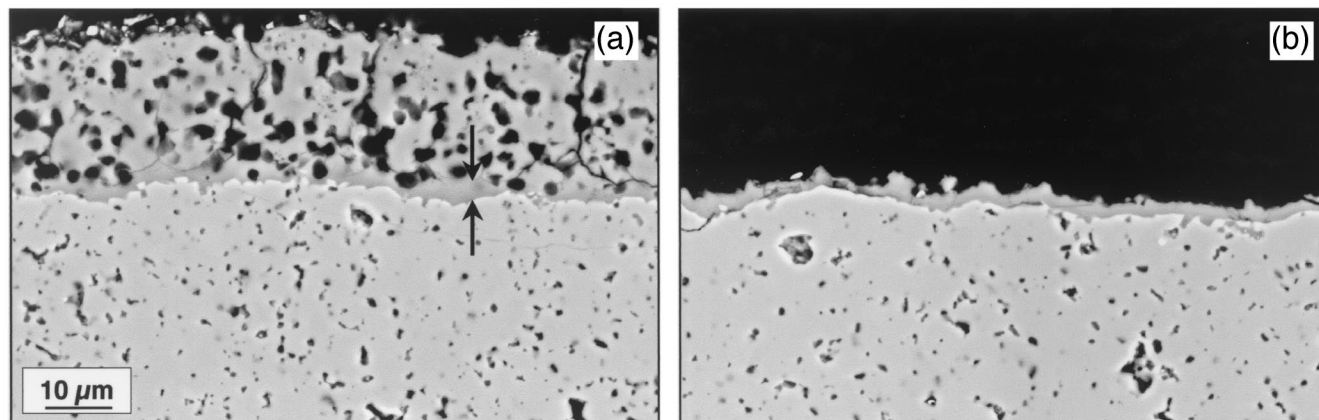


Fig. 1. SiO_2 scales on sintered α -SiC after exposure at 1200°C for 100 h at 10 atm in (a) air + 15% H_2O and (b) 100% air. Arrows in (a) denote dense vitreous SiO_2 layer.

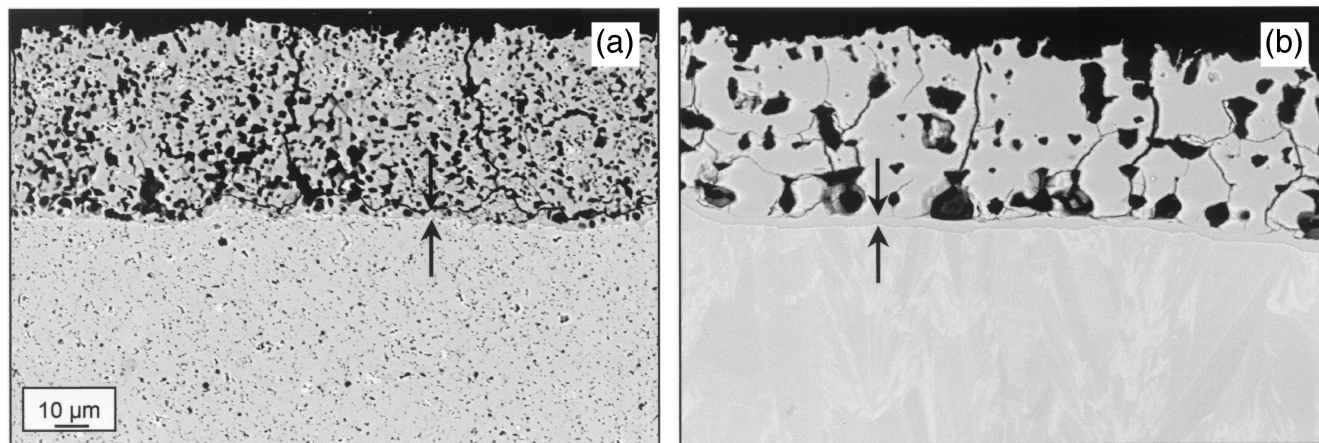


Fig. 2. SiO₂ scales formed on (a) sintered α-SiC and (b) CVD-SiC after exposure at 1200°C for 500 h at 10 atm in air + 15% H₂O. Arrows denote underlying dense vitreous SiO₂ layer.

sections of sequentially exposed specimens of sintered α-SiC and CVD-SiC. Multiple measurements were made on each cross section to determine a mean value of x (x_m); the difference between this and the starting thickness of the specimen (x_o) yielded recession data, which are plotted as $(x_m - x_o)/2$ versus oxidation time in Fig. 8. Typically, standard deviations were on the order of $\pm 30\%$ because of nonplanar oxidation fronts as well as microstructural inhomogeneities. This latter factor was significantly greater for the sintered α-SiC, which, in turn, tended to have a greater recession measurement uncertainty. Furthermore, a small, but consistent, effect of vertical position in the reaction tube was noted using a series of control experiments. The data showed that recession rates were slightly higher for specimens positioned near the bottom of the tube. This position effect was taken into account in the presentation of the recession data of Fig. 8; each data set was for specimens taken from the same position.

Despite the sources of scatter in the experimental recession data, Fig. 8 clearly indicates that the extent of oxidation is substantially greater (~ 40 – 80 μm of SiC recession in 1000 h) than what has been reported for this temperature and more modest pressures of water vapor.^{4,5,8} Furthermore, the recession distances measured in this study are much greater than what are expected for solid-state oxidation of SiC controlled by oxidant transport across a growing SiO₂ layer at 1.5 atm of water vapor. This difference is shown by comparing the experimental curves with the upper curve in Fig. 8.

The measured SiC recession at 1200°C and 10 atm of air + 1.5 atm H₂O is considerably greater than what would be predicted based on the extrapolation of Opila's determination of the functional dependence of k_p on the $p_{\text{H}_2\text{O}}$ for CVD-SiC⁸ to 1.5 atm of water vapor. Furthermore, the present recession rates are also substantially greater than what would be predicted from the parabolic kinetic formulation based on SiO₂ volatilization^{9,10} because of the very low gas-flow velocity of the current experiments (see below).

IV. Discussion

The presence of water vapor at a partial pressure of 1.5 atm had a dramatic and unique effect on the oxidation of SiC in view of the low gas-flow velocity used in this work. The total thickness of the SiO₂ that formed on SiC exposed to 8.5 atm (850 kPa) air + 1.5 atm (150 kPa) H₂O at 1200°C was always much greater than that produced during exposure to 10 atm air (~ 25 versus ~ 3 μm, respectively, after 100 h, Fig. 1). When oxygen was the major oxidant, only thin vitreous SiO₂ scales formed (Fig. 1(b)), at a rate comparable to that reported in the literature for low water-vapor pressures.⁴ This finding is consistent with the work of Deal and Grove¹ and Opila,⁸ who demonstrated that H₂O is the dominant oxidant when it is present in significant concentrations and with a finding by Keiser¹³ that substituting argon for air in an air +

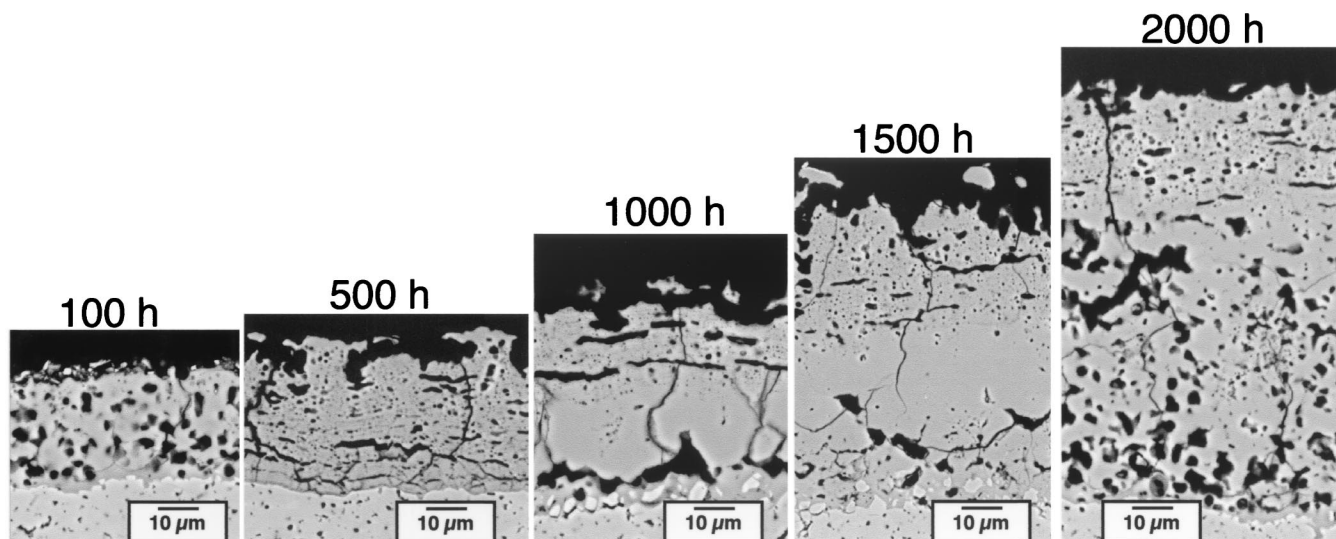


Fig. 3. SiO₂ scales on sintered α-SiC as a function of exposure time at 1200°C in 10 atm of air + 15% H₂O.

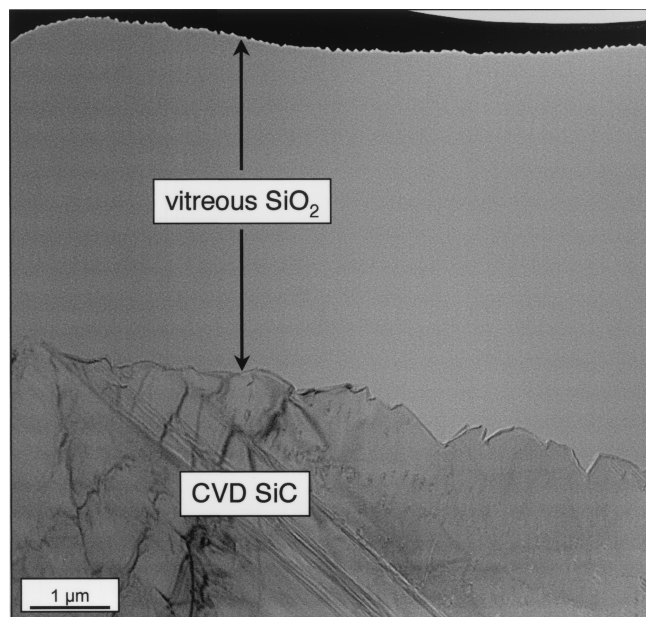


Fig. 4. Cross-sectional TEM image of the thin underlying dense layer on CVD SiC exposed for 500 h in air + 1.5 atm H₂O at 1200°C and 10 atm.

water-vapor gas mixture had little effect on oxidation of α -SiC at $p_{\text{H}_2\text{O}}$ values that were of the same order as used in the present study.

The observation of crystalline oxide after 1200°C exposures at 1.5 atm of water vapor is in contrast to the work of Opila,⁸ who observed little conversion of amorphous SiO₂ to cristobalite during exposure of CVD-SiC to 0.9 atm (900 kPa) of water vapor at 1200°C. However, studies with SiO₂-glasses have indicated that H₂O can somewhat increase the devitrification rate and lower the crystallization temperature.¹⁴ Furthermore, Opila^{5,8} has shown that water vapor facilitates the delivery of impurities from elsewhere in the system to the SiO₂ surface and, thus, increases the devitrification process. These effects can be enhanced at higher water-vapor pressures such as used in this study. More *et al.*¹² reported that the exposure of fused SiO₂ in 10 atm of air or air + 1.5 atm H₂O at 1200°C resulted in a thick surface layer of cristobalite after 100 h, but only in the presence of added water vapor. Furthermore, exposure of fused SiO₂ in air + 1.5 atm H₂O at 1200°C for 500 h showed that the converted vitreous SiO₂ (dense cristobalite, see

Fig. 9) was similar in thickness to that of the porous crystalline SiO₂ layer formed on sintered α -SiC and CVD-SiC (Fig. 2) given the respective differences in densities. A crystallization rate of $\sim 0.09 \mu\text{m/h}$ was obtained from a limited number of experiments with fused SiO₂ exposed at 1200°C in the air + 1.5 atm H₂O environment.

As described in the Introduction, it is well-known that the presence of water vapor increases the rate of SiO₂ growth on SiC at high temperature. However, as demonstrated in Fig. 8, the recession lengths measured in this study are much greater than what are expected for solid-state oxidation of SiC controlled by transport across a growing SiO₂ layer at 1.5 atm of water vapor. Therefore, the increase in SiC recession at 1200°C and 10 atm of air + 15% H₂O observed in the present case cannot be explained based only on a direct effect of water vapor on the parabolic rate constant (k_p).

Impurities in the system (such as from the furnace tube or specimen holder) can increase the oxidation rate of SiC as well as the conversion of vitreous SiO₂ to cristobalite (see above), particularly in the presence of water vapor.^{5,8} These impurity effects may contribute to the measurement of SiC recession rates that are higher than those predicted by Opila's relationship for k_p .⁸ However, such impurity effects alone cannot explain the observations reported here.

Water vapor can also accelerate SiC recession by limiting the thickness of the SiO₂ reaction product by formation of volatile Si(OH)₄.^{9,10} As reviewed in the Introduction, such a process is well described by parabolic kinetics and, at longer times, results in linear recession rates. Under these conditions, the linear rate constant (k_l) is a function of temperature, $p_{\text{H}_2\text{O}}$, and the flow velocity of the oxidizing gas for a given silicon-based ceramic.^{9,10} However, the results presented above indicate such volatilization is not a major factor: the thickness of the cristobalite layer is continually increasing with time, and the appropriate functional description for recession of SiC controlled by volatilization of SiO₂ (Ref. 9) predicts a k_l of $\sim 0.001 \mu\text{m/h}$ for the high $p_{\text{H}_2\text{O}}$, low flow velocity of the present experiments, whereas a linear fit for the data in Fig. 10 yields significantly higher measured recession rates ($\sim 0.06 \mu\text{m/h}$ for CVD-SiC and ~ 0.04 – $0.08 \mu\text{m/h}$ for sintered α -SiC). Additionally, when the gas-flow velocity was increased to 18 cm/min (from 3 cm/min) in one experiment, the effect on SiC recession was negligible.

Although SiC recession is obviously not controlled by volatilization of SiO₂ in this low-gas-velocity case, the present observations that the thin vitreous SiO₂ layer does not thicken with time suggest a process of similar parabolic kinetic form: a layer of fixed thickness is maintained as the oxidation front proceeds into

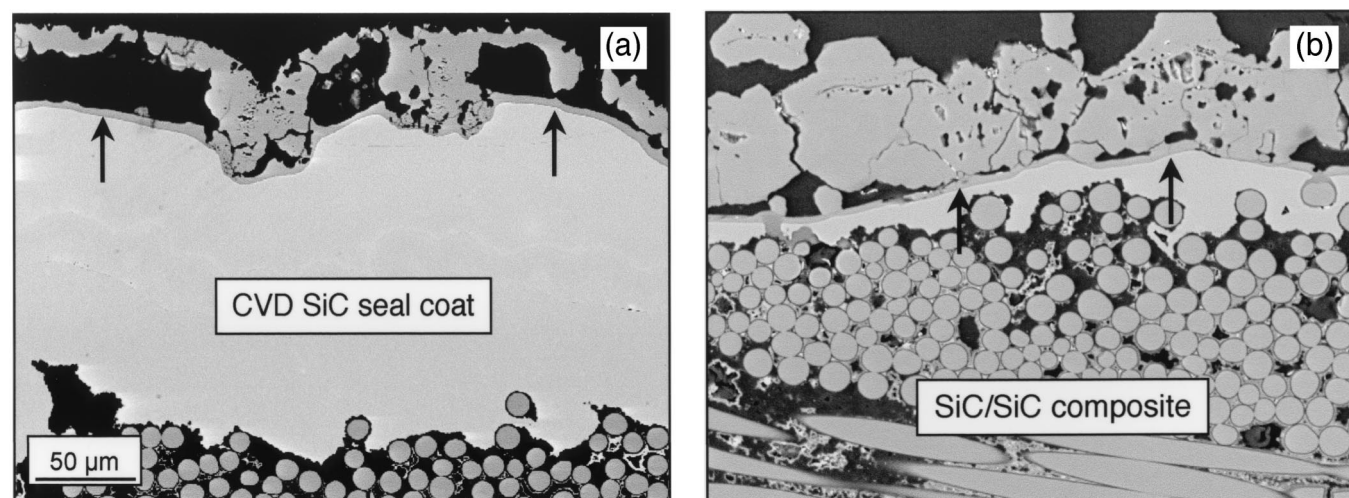


Fig. 5. SiO₂ scales formed on CVD-SiC seal-coated SiC/SiC composites after exposure in air + 15% H₂O at 1200°C and 10 atm for (a) 500 and (b) 3500 h at 1200°C.

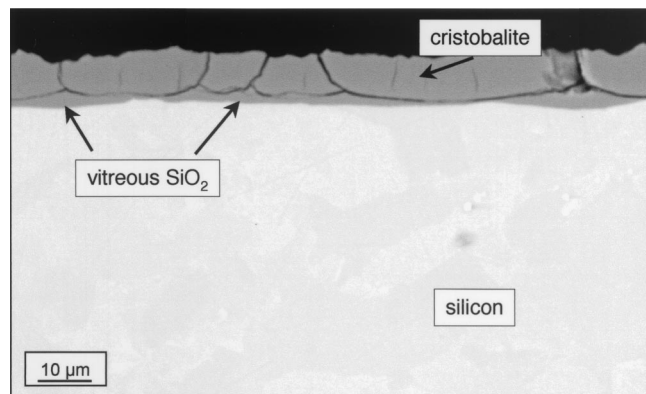


Fig. 6. SiO₂ scale formed on pure silicon after exposure at 1200°C and 10 atm for 500 h in air + 15% H₂O. Cracking in cristobalite most likely occurred during cooling.

the SiC at the same rate at which the dense SiO₂ is converted to a porous, nonprotective oxide. As such, the phenomenon functionally resembles that represented by the model of Haycock,¹⁵ who treated the kinetics of a moving boundary problem as controlled by the transformation of a compact dense scale to a porous nonprotective scale (without specifying a specific mechanism). In such a parabolic kinetic model, the invariant thickness of the dense SiO₂ (d) is proportional to the ratio of the parabolic rate constant for the solid-state oxidation of SiC to SiO₂ (k_p to k_i):¹

$$d = \frac{k_p}{2k_i} \quad (3)$$

Because the current microstructural measurements yield experimental values of d ($\sim 4 \mu\text{m}$) as well as k_i (0.06 $\mu\text{m}^2/\text{h}$ for CVD-SiC and 0.04–0.08 $\mu\text{m}^2/\text{h}$ for α -SiC), k_p can be calculated from Eq. (3). Doing so yields

$$k_p = 0.5 \mu\text{m}^2/\text{h} \text{ for CVD-SiC} \quad (4)$$

and

$$k_p = 0.3\text{--}0.7 \mu\text{m}^2/\text{h} \text{ for } \alpha\text{-SiC} \quad (5)$$

These k_p values can be directly compared with the expected value of the parabolic rate constant based on its functional dependence on temperature and $p_{\text{H}_2\text{O}}$ as determined by Opila for CVD-SiC.⁸ Using the present experimental conditions of 1200°C and 1.5 atm of water vapor, a k_p of 0.5 $\mu\text{m}^2/\text{h}$ is calculated for CVD-SiC based on Opila's work.⁸ This value agrees quite well with those derived from the experimental measurements (Eqs. (4) and (5)).

The excellent agreement between the predicted parabolic rate constant and the experimentally determined values of k_p (through its dependence on k_i and d) is strong evidence for the applicability of the parabolic kinetic model to the present case of oxidation of SiC at high water-vapor pressures and low gas-flow velocities. Furthermore, the microstructural observations of the porous outer layer are consistent with the aforementioned model of Haycock.¹⁵ As adapted in this way, this model has technological relevance for combustion conditions with respect to oxidation of SiC within a composite¹¹ or underneath a defective protective coating,¹⁶ where conditions of high water-vapor pressure and low gas velocity exist.

The experimental and analytical evidence for a parabolic kinetic model does not, in itself, yield a mechanistic explanation for the process creating nonprotective oxide, as represented by the linear recession rate described by k_i . Possibilities include the vitreous to cristobalite transformation or the dense to porous oxide transition. The latter mechanism appears more likely, because the conversion to a highly porous SiO₂ quite clearly renders the oxide nonprotective, whereas the crystallization process alone would not necessarily produce such high recession rates. In this regard,

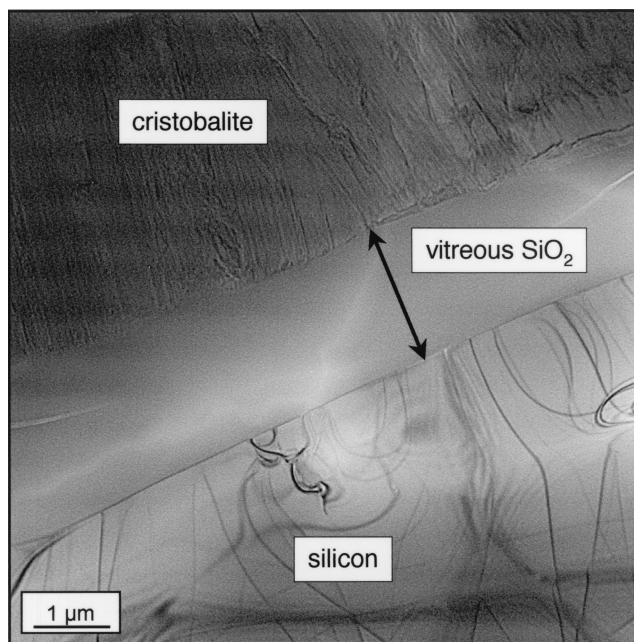


Fig. 7. Cross-sectional TEM image of the thin underlying dense layer on pure silicon exposed for 500 h in air + 15% H₂O at 1200°C and 10 atm.

although pure silicon formed cristobalite in this study (Fig. 6), it was virtually pore free, and, based on very limited data, its recession rate was less than that of the silicon carbides by a factor of ~ 3 .

Prior work in oxygen or lower pressures of water vapor^{8,17–19} and the present microstructural observations suggest that the conversion of dense to porous SiO₂ at high water-vapor pressures and low gas velocities is related to the copious amounts of CO and other gaseous reaction products associated with impurities/additives in the ceramic.^{17,20} These products are generated during the accelerated solid-state oxidation of SiC at high water-vapor pressures and then accumulate in the oxide layer. The lack of porosity

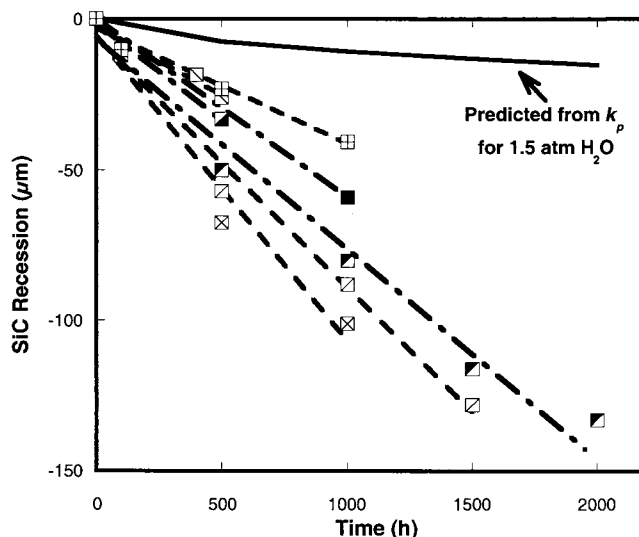


Fig. 8. SiC recession as a function of exposure time for air + 15% H₂O at 1200°C and 10 atm. Data points represent average recession and lines (black for CVD-SiC and gray for α -SiC) are best linear fits. CVD-SiC data represented by fully and partially shaded squares. Sintered α -SiC data shown as squares enclosing \times , $+$, $/$, or \backslash . Upper solid curve (no data points) is based on recession controlled by parabolic oxidation kinetics with a k_p value calculated for this temperature and gas environment using the formulation of Opila.⁸

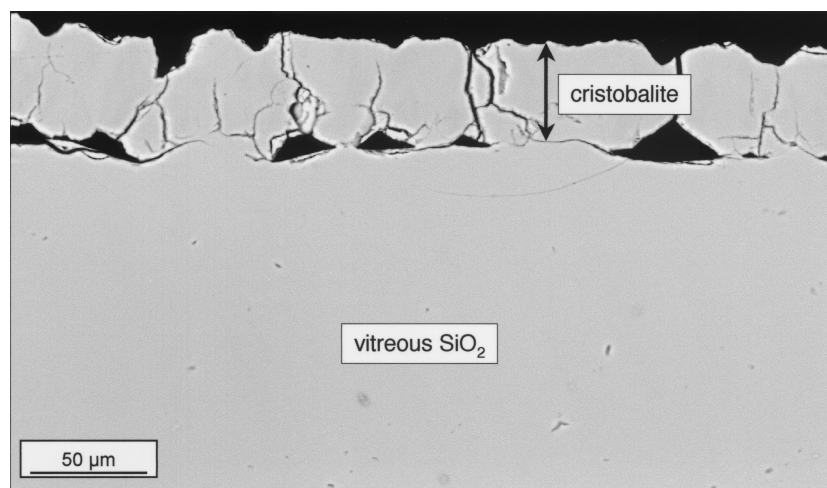


Fig. 9. Fused SiO_2 surface after exposure in air + 15% H_2O at 1200°C and 10 atm for 500 h.

in the oxide grown on pure silicon (Figs. 6 and 7) thus is explained by the fact that no such gaseous species are produced. (Hydrogen is a reaction product, but should not contribute to pore formation.) Also, the differences in the respective morphologies of the cristobalite layers grown on CVD-SiC and sintered α -SiC (Figs. 1 and 2) are consistent with a relationship between gaseous oxidation products and porosity. The observations that the sintered α -SiC has a greater amount and finer distribution of pores in the cristobalite grown on it compared with the higher-purity CVD-SiC suggest that the pore morphology appears to be directly related to the impurity/sintering-aid distribution and amount in the former material, including the influence of grain boundaries and second phases,^{17,20,21} as well as to the oxidation of excess carbon added for sintering.^{18,19} The absence of pores in the vitreous layer formed on CVD-SiC is not understood, but it may be related to relative transport rates and critical oxide thickness and concentrations of gaseous products for porosity formation in the respective silicon carbides.^{18,19} Close examination of images, such as those shown in Fig. 2, shows a distinct influence of grain structure on pore shapes and distribution. Consequently, the microstructural and impurity differences between the two types of SiC should be reflected in the evolution of porosity in the cristobalite formed on the respective materials.

The present results suggest that, at sufficiently high water-vapor pressures, a parabolic kinetic model can describe the SiC recession process at high and low gas velocities, albeit with different controlling mechanisms by which dense SiO_2 is rendered ineffective as an oxidation barrier (from removal either by volatilization or by conversion to highly defective oxide, respectively). Figure 10 compares an oxidized CVD-SiC seal coat (on a SiC/SiC composite) from the present work with a similar coating exposed at 1200°C and 1.5 atm H_2O as part of a combustor liner taken from

a gas turbine (Model Centaur 50S, Solar Turbines, Inc., San Diego, CA; see Ref. 11 for details). As expected, there was no evidence of a porous layer in the latter case; the oxidant gas velocity in the combustor was ~ 30 m/s and volatilization should be a dominant reaction.^{9,10} However, consistent with the applicability of the parabolic kinetic model at high and low gas velocities and high water-vapor pressures, a thin, dense SiO_2 layer was observed under turbine and laboratory conditions. Furthermore, Fig. 10 shows that the thickness of the SiO_2 layer on the specimens exposed under the high-gas-velocity conditions of the combustor (d_c) was about the same as that of the dense vitreous SiO_2 layers observed on the CVD-SiC held at 1200°C in air + 1.5 atm H_2O flowing at 3 cm/min (d). Referring to Eq. (3), this observation that $d_c \approx d$ would imply similar SiC recession rates (k_1 values) because k_p should be the same for both cases, as it is dependent only on temperature and water-vapor pressure. Therefore, from the information obtained from the comparison of the micrographs in Fig. 10, it is not surprising that the SiC recession rates measured in the present experiments (0.04–0.08 $\mu\text{m}/\text{h}$) are of the same order as those predicted from the SiO_2 volatilization model⁹ for the combustor liner conditions at a gas velocity of 30 m/s (0.16 $\mu\text{m}/\text{h}$).

V. Summary

Silicon carbides and pure silicon have been exposed at 1200°C and 10 atm to an air + 15% H_2O gas flowing at ~ 3 and 18 cm/min to examine the effects of high water-vapor pressures at low gas-flow velocities. Because of the nature of the reaction products that formed, it was necessary to evaluate the oxidation processes and to measure the ceramic recession rates using microstructural

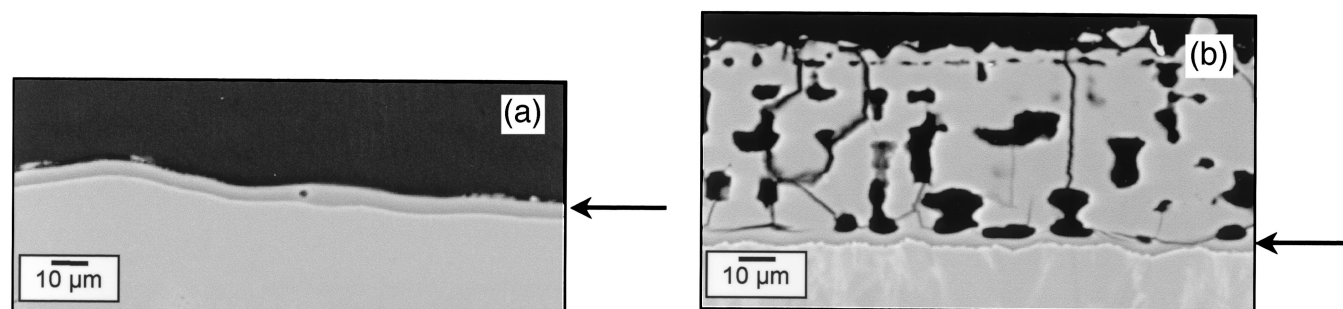


Fig. 10. CVD-SiC seal coats (on SiC/SiC composites) after exposures in 1.5 atm H_2O at the high gas velocity (~ 30 m/s) of (a) Solar Turbines combustor at $\sim 1200^\circ\text{C}$ for 5016 h and (b) low gas velocity (~ 3 cm/min) of a laboratory furnace (ORNL rig) at 1200°C after 500 h.

analysis. It was found that the high water-vapor pressure accelerated the formation of SiO_2 , the rate of its crystallization, and the amount of porosity formed in the resulting oxide. These processes resulted in measurements of SiC recession rates that were higher than what could be explained by models that relate¹ parabolic oxidation-rate constants to water-vapor pressures or² linear recession rates to gas velocity based on SiO_2 volatility. An important finding was the constant thickness of dense vitreous SiO_2 underlying the continually growing porous oxide layer. In addition, there was a distinct difference in oxide morphology among oxidized CVD-SiC, sintered α -SiC, and pure silicon. These results, as well as others, indicated that the water-vapor effect on SiC at high temperature and pressures, but low gas velocities, was manifested as a parabolic phenomenon controlled by the rapid conversion of a constant-thickness, dense, vitreous SiO_2 layer to a porous, nonprotective SiO_2 , most probably by production of gaseous oxidation products. Consequently, at sufficiently high water-vapor pressures and temperatures, relatively rapid SiC recession can occur at low and high gas velocities if SiO_2 is being produced by solid-state oxidation.

Acknowledgments

The authors thank D. W. Coffey, T. Geer, J. R. Keiser, and L. R. Walker for experimental and analytical assistance and M. P. Brady and M. K. Ferber for reviews of the manuscript. They also thank E. A. Opila and J. L. Smialek of the NASA Glenn Research Center for helpful comments and insights regarding this work.

References

- ¹B. E. Deal and A. S. Grove, "General Relationship for the Thermal Oxidation of Silicon," *J. Appl. Phys.*, **36**, 3770–78 (1965).
- ²S. C. Singhal, "Effect of Water Vapor on the Oxidation of Hot-Pressed Silicon Nitride and Silicon Carbide," *J. Am. Ceram. Soc.*, **59**, 81–82 (1976).
- ³T. Narushima, T. Goto, Y. Iguchi, and T. Hirai, "High-Temperature Oxidation of Chemically Vapor-Deposited Silicon Carbide in Wet Oxygen at 1823 to 1923 K," *J. Am. Ceram. Soc.*, **73**, 3580–84 (1990).

- ⁴N. S. Jacobson, "Corrosion of Silicon-Based Ceramics in Combustion Environments," *J. Am. Ceram. Soc.*, **76**, 3–28 (1993).
- ⁵E. J. Opila, "Oxidation Kinetics of Chemically Vapor Deposited Silicon Carbide in Wet Oxygen," *J. Am. Ceram. Soc.*, **77**, 730–36 (1994).
- ⁶J. R. Keiser, M. Howell, J. J. Williams, and R. A. Rosenberg, "Compatibility of Selected Ceramics with Steam–Methane Reformer Environments"; Paper No. 140 in *Corrosion/96*. NACE International, Houston, TX, 1996.
- ⁷E. J. Opila and R. E. Hann, "Paralinear Oxidation of CVD SiC in Water Vapor," *J. Am. Ceram. Soc.*, **80**, 197–205 (1997).
- ⁸E. J. Opila, "Variation of the Oxidation Rate of Silicon Carbide with Water-Vapor Pressure," *J. Am. Ceram. Soc.*, **82**, 625–36 (1999).
- ⁹R. C. Robinson and J. L. Smialek, "SiC Recession Caused by SiO_2 Scale Volatility under Combustion Conditions: I, Experimental Results and Empirical Model," *J. Am. Ceram. Soc.*, **82**, 1817–25 (1999).
- ¹⁰E. J. Opila, J. L. Smialek, R. C. Robinson, D. S. Fox, and N. S. Jacobson, "SiC Recession Caused by SiO_2 Scale Volatility under Combustion Conditions: II, Thermodynamics and Gaseous-Diffusion Model," *J. Am. Ceram. Soc.*, **82**, 1826–34 (1999).
- ¹¹K. L. More, P. F. Tortorelli, M. K. Ferber, L. R. Walker, J. R. Keiser, W. D. Brentnall, N. Miriyala, and J. R. Price, "Exposure of Ceramics and Ceramic-Matrix Composites in Simulated and Actual Combustor Environments," *J. Eng. Gas Turbines Power*, **122**, 212–18 (2000).
- ¹²K. L. More, P. F. Tortorelli, J. R. Keiser, and M. K. Ferber, "Observations of Accelerated Silicon Carbide Recession by Oxidation at High Water-Vapor Pressures," *J. Am. Ceram. Soc.*, **83**, 211–13 (2000).
- ¹³J. R. Keiser, Oak Ridge National Laboratory, unpublished results, 1996.
- ¹⁴H. Scholze, *Glass*, pp. 65, 84, 146. Springer-Verlag, New York, 1991.
- ¹⁵E. W. Haycock, "Transitions from Parabolic to Linear Kinetics in Scaling of Metals," *J. Electrochem. Soc.*, **106**, 771–75 (1959).
- ¹⁶K. L. More, P. F. Tortorelli, L. R. Walker, J. B. Kimmel, N. Miriyala, J. R. Price, H. E. Eaton, E. Y. Sun, and G. D. Linsey, "Evaluating Environmental Barrier Coatings on Ceramic-Matrix Composites After Engine and Laboratory Exposures"; Paper No. GT-2002–30630 in *Proceedings of the ASME Turbo Expo 2002*. ASME International, New York, 2002.
- ¹⁷S. C. Singhal, "Oxidation Kinetics of Hot-Pressed Silicon Carbide," *J. Mater. Sci.*, **11**, 1246–53 (1976).
- ¹⁸D. M. Mieskowski, T. E. Mitchell, and A. H. Heuer, "Bubble Formation in Oxide Scales on SiC," *J. Am. Ceram. Soc.*, **67**, C-17–C-19 (1984).
- ¹⁹K. L. Luthra, "Some New Perspectives on Oxidation of Silicon Carbide and Silicon Nitride," *J. Am. Ceram. Soc.*, **74**, 1095–103 (1991).
- ²⁰R. Browning, J. L. Smialek, and N. S. Jacobson, "Multielement Mapping of α -SiC by Scanning Auger Microscopy," *Adv. Ceram. Mater.*, **2**, 773–79 (1987).
- ²¹K. L. More, Oak Ridge National Laboratory, unpublished results, 1999. □